JOURNAL OF COMPUTATIONAL PHYSICS 94, 467-486 (1991)

A Stochastic Cellular Automaton Model of Non-linear Diffusion and Diffusion with Reaction

LEESA M. BRIEGER AND ERNESTO BONOMI

Ecole Polytechnique Fédérale de Lausanne, CH-1015 Lausanne, Switzerland

Received July 19, 1989; revised February 23, 1990

This article presents a stochastic cellular automaton model of diffusion and diffusion with reaction. The master equations for the model are examined, and we assess the difference between the implementation in which a single particle at a time moves (asynchronous dynamics) and one implementation in which all particles move simultaneously (synchronous dynamics). Biasing locally each particle's random walk, we alter the diffusion coefficients of the system. By appropriately choosing the biasing function, we can impose a desired non-linear diffusive behaviour in the model. We present an application of this model, adapted to include two diffusing species, two static species, and a chemical reaction in a prototypical simulation of carbonation in concrete.

1. INTRODUCTION

The construction of a computer simulation of a physical phenomenon has begun traditionally with a mathematical model consisting of differential equations defined in the continuum. This is followed by the definition of an algorithm, or numerical model, to discretize and numerically solve the equations. Finally, the numerical model is implemented on a computer, yielding the computer simulation and the numerical results which are studied to demonstrate, predict, or clarify the phemonenon in question. Of note is the fact that the final computer model is several approximations removed from the original: the numerical schema approximately solves the equations of the mathematical model, and, because of the round-off inherent in floating-point calculations, the computer implementation is itself only an approximation of the numerical model. (In fact, a principal concern in the field of numerical analysis is the quality of these approximations, i.e., assuring that the final numerical solutions generated by the computer are faithful to the true solution of the original mathematical model.)

Cellular automata offer an alternative to this approach to modelling [1]. In a cellular automaton model, space is discretized by a lattice whose grid points (sites) are permitted a finite number of values (states). The state of each site evolves step by step in the model. This evolution is governed by a set of local microscopic laws (rules), identical at all the sites and which, if chosen properly, produce in the model the macroscopic behaviour to be simulated. The rules can be implemented as logi-

0021-9991/91 $3.00

cal functions performed between bits representing the states of the sites, in which case the machine implementation entails no approximation of the model but is exact. The results are then the direct image of the model, illustrating its behaviour without the additional influence of approximative numerical methods. Because of this and due to their local nature, cellular automata are also easier to adapt so as to increase the complexity of the model. Currently, modern computing capacity and special machine architecture render cellular automata practical for large numerical simulations. The intrinsic granularity of the resulting algorithms leads naturally to their implementation on vector and parallel machines [2], and machine architecture tailored to the large number of site-by-site calculations of cellular automata dynamics has given rise to one class of dedicated machines [3, 4]. The development of parallel and dedicated computers is motivating the design of numerical algorithms which exploit special machine structure. Cellular automata can be viewed as such a class of special-purpose algorithms, and investigation of them as methods for solving differential equations has begun [5–7].

The philosophy behind modelling with cellular automata is to implement local conservative microscopic laws and thus simulate the deterministic macroscopic behaviour of a physical system [8]. Although the micro-laws may be artificial, they must capture the essential global features of the system. The micro–macro connection is not obvious and it can be difficult to design local laws whose dynamics reproduce the appropriate cooperative behaviour. With this in mind, we have taken advantage of the well-established relation between the random walk of a Brownian particle and the diffusion equation [9] to develop a stochastic cellular automaton model for the simulation of diffusion, linear and non-linear. In our application we further consider diffusion with reaction in a porous medium to simulate the carbonation of concrete, a corrosive process which occurs in the presence of drying [10].

We have first implemented the random walk simulation, adapted to a population of Brownian particles which respect an exclusion principle, to model simple linear diffusion. We study the global behaviour corresponding to the basic rules of the simulation, given in Section 2, by examining the master equations for the model. We thus assess the qualitative difference between the asynchronous implementation in which a single particle at a time moves and our synchronous one in which all particles move simultaneously and independently. The synchronous model, while embodying a massively parallel algorithm, exhibits a light deviation from the true diffusion equation.

To approximate non-linear diffusion, we alter the particles' displacement probabilities by introducing a bias imposed by a given diffusion coefficient. This forces the appropriate diffusive behaviour on the system. The deviation from true diffusion, produced by our synchronous model and described in Section 2, remains present in the non-linear case. This is described in more detail in Section 3, in which we also introduce units into our heretofore dimensionless automaton model.

In Section 4 we present an adaptation of the original diffusion model, introducing two diffusing species, two static species, and a chemical reaction in a proto-

typical simulation of carbonation in concrete. Increasing the complexity of a cellular automaton simulation is simpler than the same adaptation for a traditional mathematical model, in which changes in the equations must be accompanied by an adaptation of the numerical method that solves them. In the automaton model there is no associated numerical schema, and changes in the model are implemented directly in the local rules.

2. The Automaton Model

The model of Brownian motion provided by the random walk of a particle on a square lattice is defined by a simple local rule: displace the particle with equal probability ($\frac{1}{4}$) in any one of the four directions on the lattice. This defines a probability distribution, $P(x_{ij}, t_n)$, discrete in time and space, which is just the probability that position x_{ij} is occupied by the Brownian particle at time t_n. Δt represents the time interval between consecutive steps of the particle and Δx the grid discretization. $P(x_{ij}, t_n)$ evolves diffusively on the lattice [9], and as Δx and Δt approach zero, such that the ratio $D = \Delta x^2/4\Delta t$ remains constant, $P(r, t)$ solves the following continuous diffusion equation (Fick's law of diffusion) in which D is the (constant) diffusion coefficient, and ∇^2 indicates the Laplacian operator:

$$\frac{\partial P(r, t)}{\partial t} = D\,\nabla^2 P(r, t). \tag{1}$$

The diffusive character of the displacement rule is seen clearly in the master equations for the model. The process is Markovian and the probability P_r^{n+1} that the particle occupies site $r = x_{ij}$ at time t_{n+1} is given as a function of the neighboring probabilities as time t_n by the following expression:

$$P_r^{n+1} = \sum_{q \in \mathcal{N}(r)} P_q^n W_{qr}^n. \tag{2}$$

$\mathcal{N}(r)$ is the five-site von Neumann neighborhood of r (r and its nearest neighbors on the grid), and W_{qr}^n denotes the conditional probability of moving from site q to site r at time t_n. $W_{qr}^n = 0$ whenever q and r are not in the same neighborhood, and the following conservation condition is respected:

$$\sum_{r \in \mathcal{N}(s)} W_{sr}^n = 1. \tag{3}$$

Solving for W_{rr}^n in (3), we use this to rewrite (2) and obtain the following description for the evolution of P:

$$P_r^{n+1} - P_r^n = \sum_{\substack{q \in \mathcal{N}(r) \\ q \neq r}} P_q^n W_{qr}^n - P_r^n \sum_{\substack{q \in \mathcal{N}(r) \\ q \neq r}} W_{rq}^n. \tag{4}$$

In the random walk model for one particle, the conditional probabilities for $q \in \mathcal{N}(r)$ are

$$W_{qr}^{n} = \begin{cases} \frac{1}{4}, & q \neq r \\ 0, & q = r. \end{cases} \tag{5}$$

Consequently, expression (4) takes the form

$$P_r^{n+1} - P_r^n = \frac{1}{4}\left[\sum_{\substack{q \in \mathcal{N}(r) \\ q \neq r}} P_q^n - 4P_r^n \right], \tag{6}$$

which is the finite difference representation of diffusion equation (1), using the central difference approximation to the second derivative and in which

$$D = \frac{\Delta x^2}{4\Delta t}.$$

Thus the random walk model reproduces the finite difference approximation of diffusion equation (1) on the grid. As the discretization goes to zero, with D constant, the finite difference solution converges to the solution of the continuous equation.

In our model we adapt the stochastic rule to a population of particles. The rule is applied identically at all the sites, determining the particle displacements. Each particle effectively chooses at random a direction on the square lattice, targeting one of its four neighbors. Our rule imposes an exclusion principle which permits at most one particle per site in the following way: a particle moves to the site it has targeted if this site is free and simply does not move if the site is already occupied. We consider two implementations of these dynamics for a population of particles: an asynchronous one, in which a single particle at a time moves; and a synchronous one, in which the entire population of particles is updated simultaneously and independently.

At each step in the asynchronous case, the local rule is applied at a single site, chosen at random from the N sites of the configuration. A "sweep" of the configuration is a collection of N such events. For large N the random choice of a site at which an event will occur is comparable to a Poisson clock which orders the events on the configuration. To see this, consider an arbitrary site in the configuration and define a success as the choice of this site for an event. Beginning with the last success at this site, consider the probability of no success occurring again in M sweeps; for large N this probability is approximated by the exponential e^{-M}. In this context, the partition function $F(M)$, the probability of at least one success during M sweeps, is governed by the law of Poisson, $F(M) = 1 - e^{-M}$. From this expression we deduce that there is, on average, one sweep between successes at a given site, and that, on average, each site is chosen once during a configuration sweep.

Now consider the master equations for this model. If we consider the time interval from t_n to t_{n+1} of a single event, the evolution of probability P is given by (4),

due to the Markovian nature of the process. Here the probability of transition of a particle from q to r in the space of a single event at time t_n is as follows:

$$W_{qr}^n = \frac{1}{4N}(1 - P_r^n), \qquad q \in \mathcal{N}(r),\ q \neq r. \tag{7}$$

Using these probabilities in (4), we derive the following expression for the evolution of P:

$$P_r^{n+1} - P_r^n = \frac{1}{4N}\left[\sum_{\substack{q \in \mathcal{N}(r) \\ q \neq r}} P_q^n - 4P_r^n\right]. \tag{8}$$

This is just the finite difference form of diffusion equation (1) with

$$D = \frac{\Delta x^2}{4N\,\Delta t}.$$

We conclude that in the asynchronous automaton, the particle population diffuses on the lattice, and the model reproduces the solution of the discrete approximation of diffusion equation (1), Fick's equation. We consider now a synchronous alternative.

In the synchronous model, for which a timestep $\Delta t = t_{n+1} - t_n$ is the time interval of a configuration update, conflicts between particles vying for a single free site must be resolved. In our implementation, only one of the competing particles, chosen randomly from among them, is allowed to move to the unoccupied site, and the others do not move. This induces interactions between particles beyond just the immediate neighborhood. To characterize the resulting correlations, we can write the transition probabilities as

$$W_{qr}^n = \tfrac{1}{4}(1 - P_r^n)\,A_{qr}^n, \qquad q \in \mathcal{N}(r),\ q \neq r, \tag{9}$$

where A_{qr}^n represents the conditional probability that the transition from q to r is admissible, that is, that site r accepts the particle transition from site q. With these probabilities of transition, Eq. (4), describing the evolution of P, becomes:

$$P_r^{n+1} - P_r^n = \frac{1}{4}\left[\sum_{\substack{q \in \mathcal{N}(r) \\ q \neq r}} P_q^n A_{qr}^n - P_r^n \sum_{\substack{q \in \mathcal{N}(r) \\ q \neq r}} A_{rq}^n\right] + \frac{1}{4} P_r^n \sum_{\substack{q \in \mathcal{N}(r) \\ q \neq r}} P_q^n (A_{rq}^n - A_{qr}^n). \tag{10}$$

If the automaton rule for the synchronous implementation were to produce a function A such that everywhere $A_{qr}^n = A_{rq}^n$, then the term in brackets would be diffusive with a diffusion coefficient represented by A (see Section 3), and the second term

would vanish, reproducing the finite difference form of Fick's equation. This is not the case for our synchronous rule, and our model retains some deviation from pure diffusion.

To illustrate the disparity between Fick's diffusion and this synchronous model, we consider in detail the one-dimensional case in which particles move left or right with probability $\frac{1}{2}$, respecting the exclusion principle. The one-dimensional neighborhood $\mathcal{N}_j$ of site r_j consists of sites r_{j-1}, r_j and r_{j+1}, and the transition probabilities W_{ij} corresponding to (9) are

$$W_{ij}^n = \tfrac{1}{2}(1 - P_j^n)\, A_{ij}^n, \qquad i = j-1, j+1, \tag{11}$$

where

$$A_{j-1,j}^n = 1 - \tfrac{1}{4} P_{j+1}^n$$
$$A_{j+1,j}^n = 1 - \tfrac{1}{4} P_{j-1}^n.$$

The dynamics are still Markovian and Eq. (4) describes the probability evolution, which takes the form with the transition probabilities of (11),

$$P_j^{n+1} - P_j^n = \frac{1}{2}\left[\sum_{\substack{i \in \mathcal{N}(j) \\ i \neq j}} P_i^n - 2P_j^n\right] + E_j^n, \tag{12}$$

where

$$E_j^n = \tfrac{1}{8}\{P_{j-2}^n(1 - P_{j-1}^n)\, P_j^n - 2P_{j-1}^n(1 - P_j^n)\, P_{j+1}^n + P_j^n(1 - P_{j+1}^n)\, P_{j+2}^n\}.$$

Equation (12) is the one-dimensional finite difference form of diffusion equation (1) with

$$D = \frac{\Delta x^2}{2\Delta t}$$

plus the "correction" term E_j^n, which, for uniform populations (P constant), is zero. The effect of this extra term on the simulation is illustrated in an example of one-dimensional diffusion at equilibrium, Fig. 1. The diffusion equation

$$\frac{\partial u}{\partial t} = \frac{1}{2}\frac{\partial^2 u}{\partial x^2} \qquad \text{with} \quad \begin{cases} u(0, t) = 0 \\ u(1, t) = 1 \end{cases} \tag{13}$$

has equilibrium solution $u(x, t) = x$ on the unit interval. Constraining the automaton dynamics to one dimension, we use the synchronous model to conduct 100 simultaneous one-dimensional simulations of this problem on the two-dimensional grid. The initial density of the particles on the two-dimensional lattice is distributed so as to correspond to the equilibrium solution of problem (13), the dashed line in the figure. The steady state of the model is shown in Fig. 1: the smooth curve is the fixed point of the numerical iteration defined by (12), with $P(x, 0) = x$, and the "experimental" points are the measurements of the average particle distribution, as a function of x, over the 100 automaton experiments, at

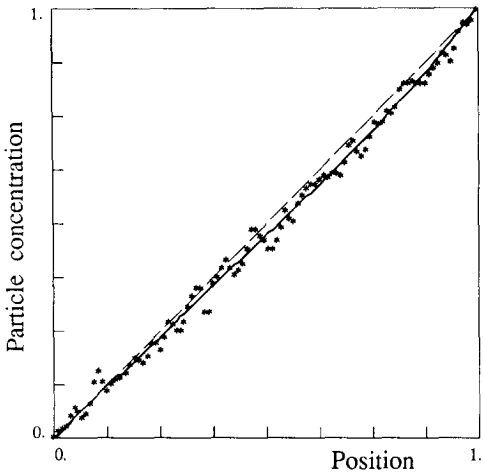

FIG. 1. Law of Fourier. The dashed line is the steady-state solution of Eq. (13). The solid curve is the exact concentration at equilibrium for the synchronous automaton; i.e., it is the fixed point of the numerical iteration defined by Eq. (12). The *'s indicate the automaton concentration measurements at equilibrium (timestep 20,000).

timestep 20,000. Equilibrium for the synchronous system is not the straight line equilibrium solution of (13), nor does it approach the straight line as the discretization is made increasingly fine. The effect of the competition for free sites is to introduce a form of "hardcore interactions" and to slightly inhibit the diffusion.

In general, finding the right microscopic automaton rules for correctly reproducing a given equation is a problem with no immediate answer; there is no methodology leading to its solution. For the moment, it is probably a combination of physical principles and intuition that will give the automaton model corresponding to a desired macroscopic behaviour. This problem is illustrated by the difficulty of defining a probabilistic synchronous model for simulating the diffusion equation without spurious effects.

Although the asynchronous dynamics more closely reproduce Fick's equation of diffusion, it is the synchronous model which holds the interest as a massively parallel algorithm, and it is on the synchronous model that we have concentrated our practical efforts. The figures in this article are all "snapshots" of the synchronous implementation.

3. NON-LINEAR DIFFUSION

Equation (1) in Section 2 is an example of Fick's law of diffusion in the special case of a constant coefficient D. Non-uniform diffusion, as in a porous medium, can also be modelled by Fick's equation:

$$\frac{\partial u}{\partial t} = \operatorname{div}(\mathscr{D} \cdot \mathbf{grad}\, u) \tag{14}$$

in which the coefficient $\mathscr{D}$ is a positive function of position or of the solution. Fick's law remains the physical model of the phenomenon, in which the interacting influences of porosity and fluid characteristics [11] are described by an effective diffusion coefficient which captures the phenomenology and governs the model accordingly. The coefficient can be supplied either from theoretical considerations or from experimental observations, and when it is a function of the solution u, Eq. (14) is non-linear. Drying in concrete modelled as non-linear diffusion, studied in [12] and applied in [13], represents an application of such an approach.

We have adopted this approach for our automaton model of diffusion in a porous medium. We have chosen not to recreate in the automaton the detailed microscopic processes which produce diffusion; rather, we have constructed a model which simulates the non-linear diffusion equation. Assuming the diffusion coefficient given, we use it to influence the displacement probabilities in the automaton in such a way as to reproduce the effect of the coefficient and the behaviour of Eq. (14).

The idea and the algorithm are as follows. In two dimensions, rather than choosing its displacement direction with probability $\frac{1}{4}$, a particle targets a direction with probability $\frac{1}{4}D$, where D is a given function which can be evaluated on the lattice. We denote by D_r^n the function D evaluated at site r at moment t_n and by D_{qr}^n the arithmetic average of D_q^n and D_r^n, $D_{qr}^n = (D_q^n + D_r^n)/2$. Then we use this value of D on the lattice edges to bias the displacement probabilities: a particle at site q chooses to move in the direction of neighboring site r with probability $\frac{1}{4}D_{qr}^n$. Notice that $0 \leqslant D \leqslant 1$ must hold since D serves as a probability, and that by using such a function to bias a particle's random walk, we introduce a non-zero probability that the particle choose not to move. The transition probabilities for such an asynchronous model with N sites are the following:

$$W_{qr}^n = \frac{1}{4N} D_{qr}^n (1 - P_r^n), \qquad q \in \mathscr{N}(r), q \neq r. \tag{15}$$

As before, Eq. (4) describes the evolution of the occupation probability at a site r. Since D is constant on each lattice edge, $D_{qr}^n = D_{rq}^n$, (4) takes the following form:

$$P_r^{n+1} - P_r^n = \frac{1}{4N} \left(\sum_{\substack{q \in \mathscr{N}(r) \\ q \neq r}} P_q^n D_{qr}^n - P_r^n \sum_{\substack{q \in \mathscr{N}(r) \\ q \neq r}} D_{qr}^n \right). \tag{16}$$

FIG. 2. Non-linear diffusion in the synchronous automaton. (a) The diffusion coefficient $\mathscr{D}$ versus the concentration u. The smooth curves show a finite element solution of Eq. (14) in one dimension at the indicated times. The experimental points are the "snapshot" automaton concentrations, measured at the same moment of simulated time.

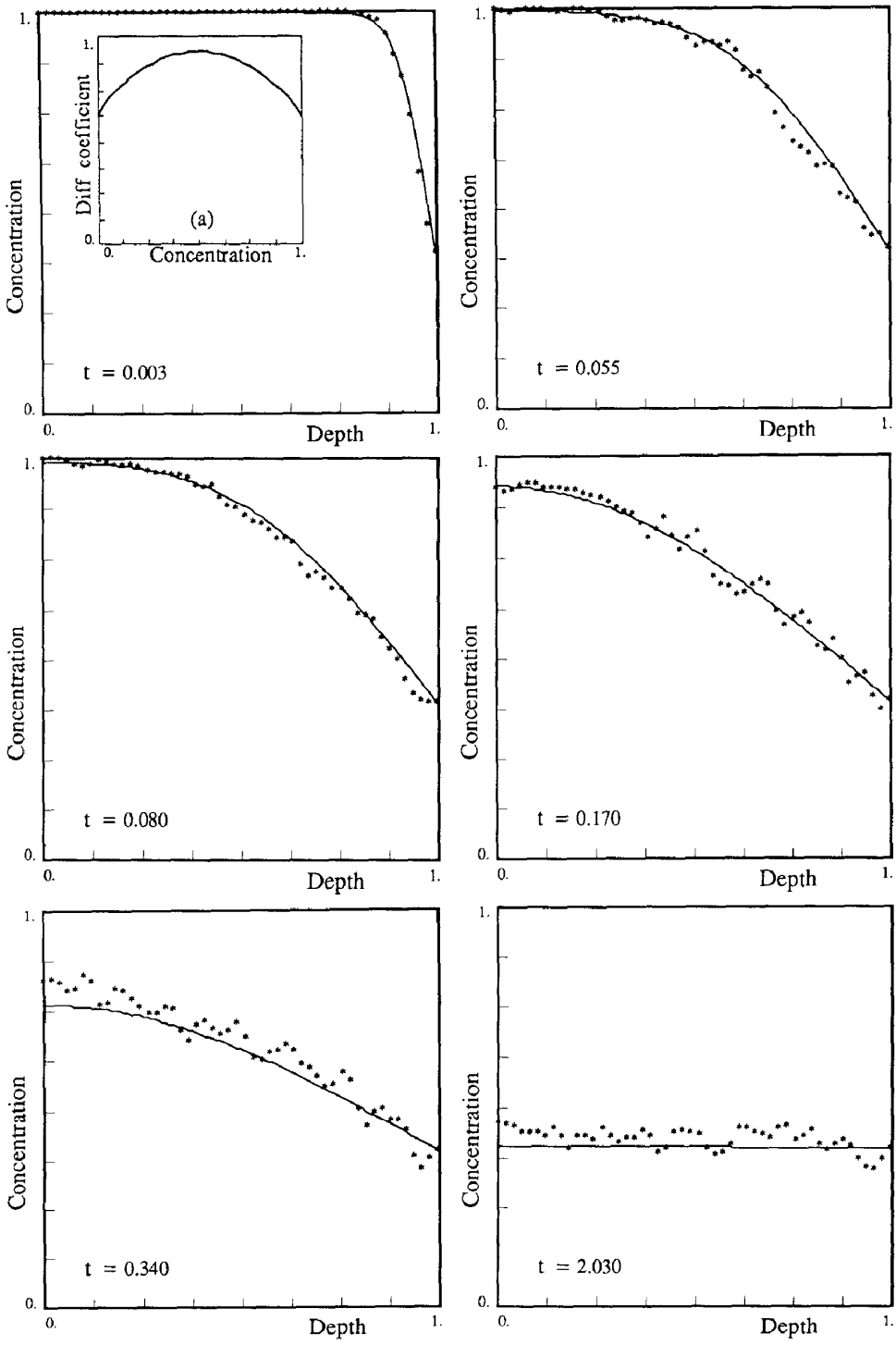
Concentration
Depth
t = 0.003
Diff coefficient
Concentration
(a)
t = 0.055
t = 0.080
t = 0.170
t = 0.340
t = 2.030
0.
1.

Equation (16) is the finite difference formulation on the square lattice of Eq. (14), with

$$\mathscr{D} = \frac{\Delta x^2}{4N\,\Delta t} D.$$

Thus, given a diffusion coefficient $\mathscr{D}$, we can implement it, to within a scaling constant, in the automaton and reproduce the corresponding non-linear diffusive behaviour in the particle population.

When $\mathscr{D}$ is a function of the solution u, D must be evaluated site-by-site as a function of the occupation probability P, which is just the local average occupation number. In this article we approximate this average by the particle concentration in a neighborhood. Notice that a particle count on the five-site von Neumann neighborhood gives only six possible values of the particle concentration. Enlarging the neighborhood on which a concentration is measured increases the number of possibilities, as does using a weighted particle count. The experiment of Fig. 2 was run with local concentrations calculated on the Moore neighborhood (the von Neumann neighborhood plus the corners) with weights of $\frac{1}{4}$, $\frac{1}{8}$, and $\frac{1}{16}$. The automaton rule was not changed; i.e., particle movement remained restricted to the five-site von Neumann neighborhood. The result is a finer representation of the diffusion coefficient and a smoothing of the concentration distributions shown in the figure.

Figure 2 shows a comparison between our synchronous automaton results and a finite element solution for non-linear diffusion equation (14) in one dimension, with the coefficient $\mathscr{D}$ a function of u as shown. The two-dimensional automaton configuration, implemented with a fixed boundary condition along $x = 1$ and zero flux conditions along the other borders, is given a one-dimensional representation by plotting the column-by-column average concentration as a function of x. The smooth curves show the finite element solution of the one-dimensional equation at the indicated times, and the experimental points are the "snapshot" automaton concentrations, measured at the same moment of simulated time. The effect of the discrepancy between Fick's equation (14) and the master equations of the synchronous model (described in Section 2) is apparent in the figure for intermediate values of the solution.

Such a comparison as that of Fig. 2 necessitates that we introduce units into the heretofore dimensionless automaton. The finite difference form of Eq. (14) for arbitrary $\mathscr{D}$ can be written as

$$u_r^{n+1} - u_r^n = \frac{k\,\Delta t}{\Delta x^2}\left(\sum_{\substack{q \in \mathcal{N}(r) \\ q \neq r}} u_q^n D_{qr}^n - u_r^n \sum_{\substack{q \in \mathcal{N}(r) \\ q \neq r}} D_{qr}^n \right), \tag{17}$$

where k is a normalization constant and $\mathscr{D} = kD$, $0 \leqslant D \leqslant 1$. If the time-space discretizations respect the relation

$$\Delta t = \frac{1}{4Nk} \Delta x^2 \tag{18}$$

and D is the function implemented in the automaton model, then Eq. (17) corresponds exactly to balance equation (16) of the automaton. Δx represents the discretization of the spatial domain by the model. The interval Δt represents the simulated time elapsed during one event of the asynchronous automaton. We can also use this to define the time elapsed with one step of the synchronous model, that is, for one configuration sweep (N events):

$$\Delta t = \frac{1}{4k} \Delta x^2. \tag{19}$$

Having calibrated the cellular automaton model with respect to simple diffusion, it is useful and straightforward to expand the model and increase its complexity. Figures 3 and 4, showing the two-dimensional automaton configurations and the corresponding one-dimensional population distributions, are examples of two such extensions of the model. Figure 3 follows the evolution of the probabilistic automaton model of a system with two inter-diffusing, non-reacting species, A and B. The system is closed (zero flux conditions on all four sides) and the two species are initially separated by a membrane which is removed at time 0. While the implemented rule is linear with a constant diffusion coefficient, the resulting cooperative dynamics produce non-linear diffusion between the two populations. Figure 4 shows the evolution of the system in which the two diffusing species, A and B, are reactive, producing a third, stationary species, C:

$$A + B \rightarrow C. \tag{20}$$

The initial configuration contains no particles of C, and A and B are initially separated by a membrane. With the removal of the membrane, the diffusion-controlled reaction begins, and the closed system evolves a distribution of C.

4. Diffusion with Reaction: Carbonation

We now consider the application of the model to a more complex problem: the simulation of a diffusion-driven reaction in a porous medium, concrete [13].

The carbonation of concrete is a corrosion process provoked by the drying of the concrete and its exposure to air which contains carbon dioxide, CO_2. The CO_2, entering concrete pores which have been emptied by drying, reacts with calcium hydroxide, $Ca(OH)_2$, present in the concrete as a hydration product. The reaction forms calcium carbonate, $CaCO_3$, and liberates water in a series of reactions usually represented simply as:

$$CO_2 + Ca(OH)_2 \rightarrow CaCO_3 + H_2O. \tag{21}$$

The carbonation reaction normally moves inward at the rate of millimeters per decade, depending on such factors as the porosity of the concrete, its $Ca(OH)_2$

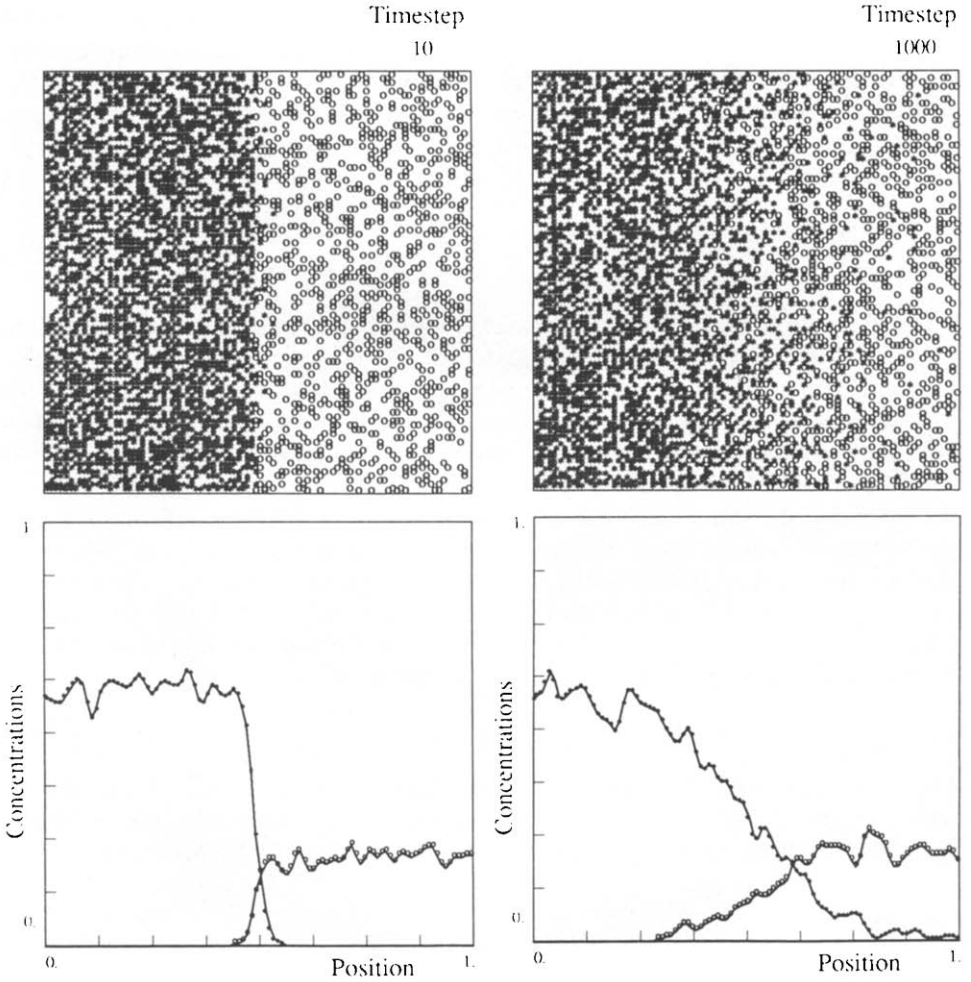

FIG. 3. Two-species inter-diffusion. Linear diffusion dynamics (D constant) drive the two populations, $A(*)$ and $B(\circ)$, which are initially separated by a membrane. The resulting interactions give rise to non-linear behaviour of the two species. Shown are the configurations of the model at the times indicated and the corresponding one-dimensional distributions of the two species.

content, atmospheric relative humidity and exposure to wetting-drying cycles, cracking, surface treatment, etc. In water-saturated conditions the carbonation front does not advance at all and one witnesses a buildup of $CaCO_3$ at the surface. Under "normal" conditions, the reaction proceeds inward, transforming $Ca(OH)_2$ into $CaCO_3$ as it goes. This transformation, once complete, lowers the pH of pore water to a level below that which protects interior steel reinforcements from corrosion. The "carbonated zone," the surface layer in which the $Ca(OH)_2$ has been exhausted and the pH diminished, progresses inward with the diffusion of the CO_2,

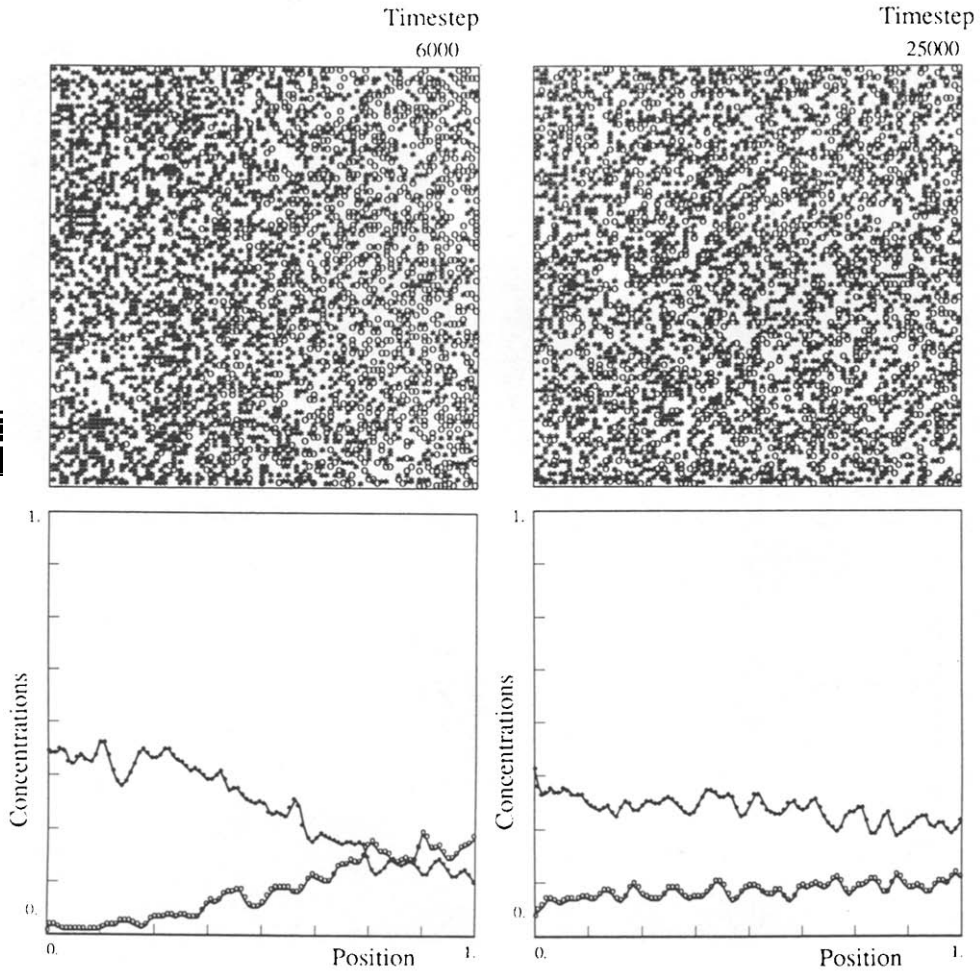

FIG. 3—*Continued*

threatening the integrity of interior reinforcements once it reaches them. To date, there is no adequate mathematical model which furnishes a macroscopic description of the various interacting factors and their influence on the carbonation environment.

We begin here the development of an automaton model of carbonation, based on the stochastic model of diffusion presented in the preceding sections. The adaptation of the original model to include several species and a chemical reaction is relatively simple. Of considerable importance is the fact that there is no accompanying numerical method which must be redefined and implemented in order to solve the revised model. In the following we give an illustration of the cellular automaton as a simulation tool rather than a systematic study of carbonation.

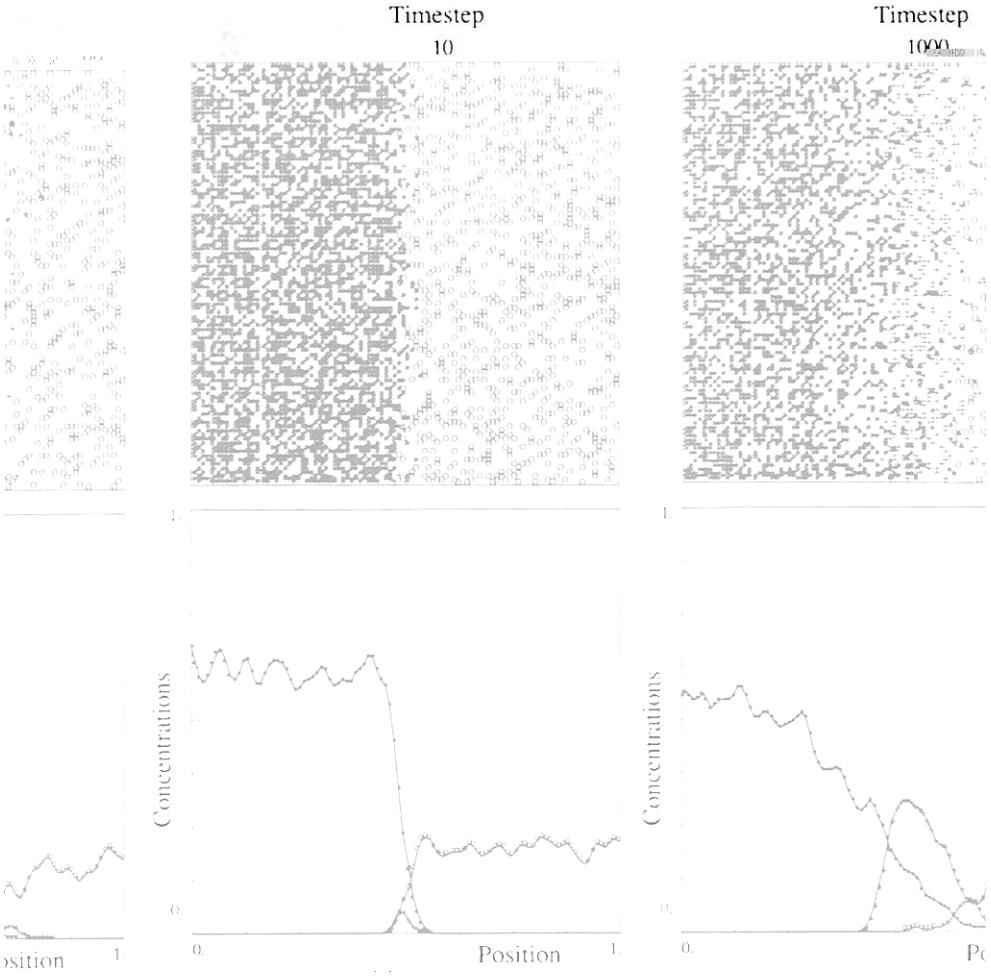

FIG. 4. Diffusion with reaction, $A + B \rightarrow C$. Populations $A(*)$ and $B(\circ)$, initially separated by a membrane, diffuse and react, forming the product $C(+)$. Shown are the configurations of the model at the times indicated and the corresponding one-dimensional distributions of the three species.

In the automaton simulation, CO_2 and H_2O are modelled as two populations of diffusing particles obeying the exclusion principle (never more than one diffusing particle per site). The movement of each population on the automaton lattice is governed by a diffusion coefficient furnished by experimental observations and representative of these fluids in the porous medium. Both diffusion coefficients are functions of the amount of water present in the concrete, giving a non-linear character to the diffusion system [12]. $Ca(OH)_2$ and $CaCO_3$ are supposed held in the pore walls and hence are represented as stationary populations of fixed particles in the background. The carbonation reaction occurs whenever the random walk of

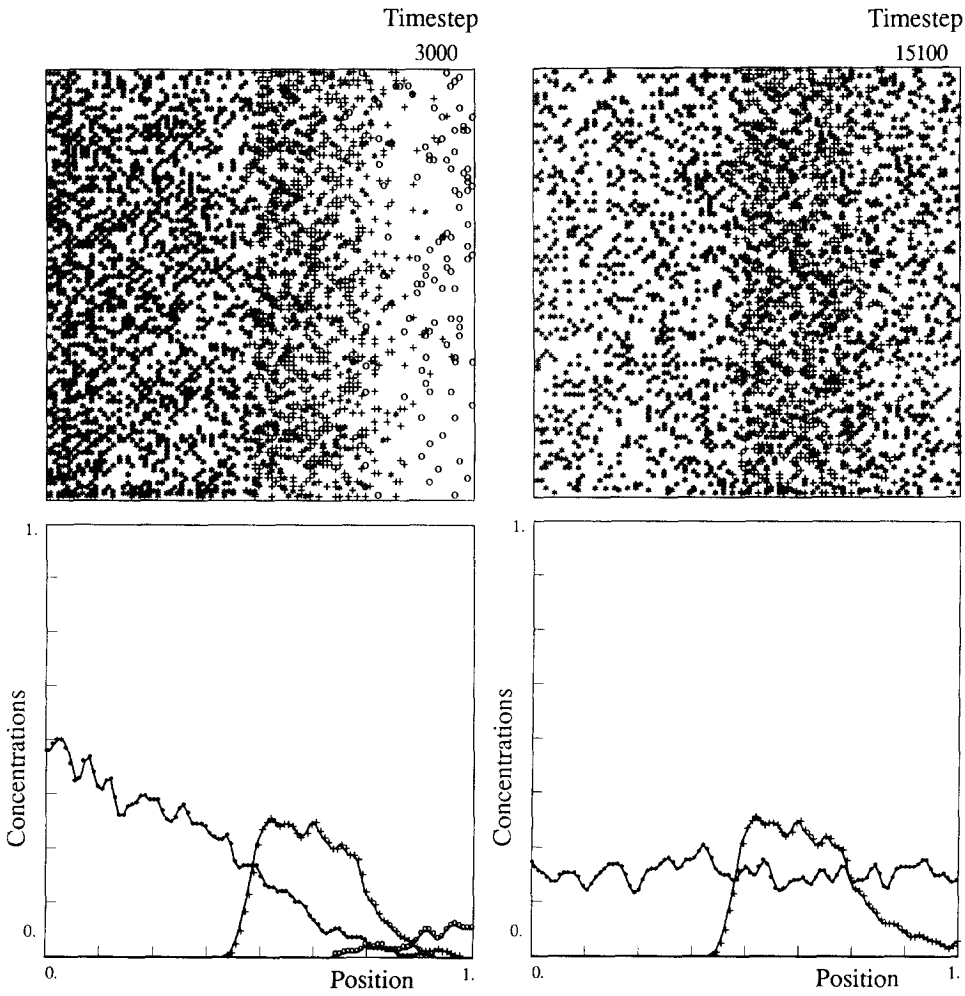

FIG. 4—*Continued*

the CO_2 produces a collision with a $Ca(OH)_2$ particle, provoking the spontaneous transformation of these two species according to (21).

Units of time simulated by the automaton are dictated by relation (19), $k = 10^{-4}$ mm^2/s, $\Delta x = 2$ mm (a sample width of 100 mm and 50 intervals in the automaton). Total water content in a porous material, at a given atmospheric relative humidity, depends on the pore size distribution of the material. Empirical curves, the sorption isotherms, relate the total water content per unit volume to relative humidity, for given pore distributions, in hardened cement pastes [14, 15]. The number of moles per cubic millimeter represented by a particle in the automaton is calibrated using the sorption isotherm for water corresponding to the porosity of the material studied: $3{,}6 \times 10^{-5}$ moles/mm^3 in this case. This choice of

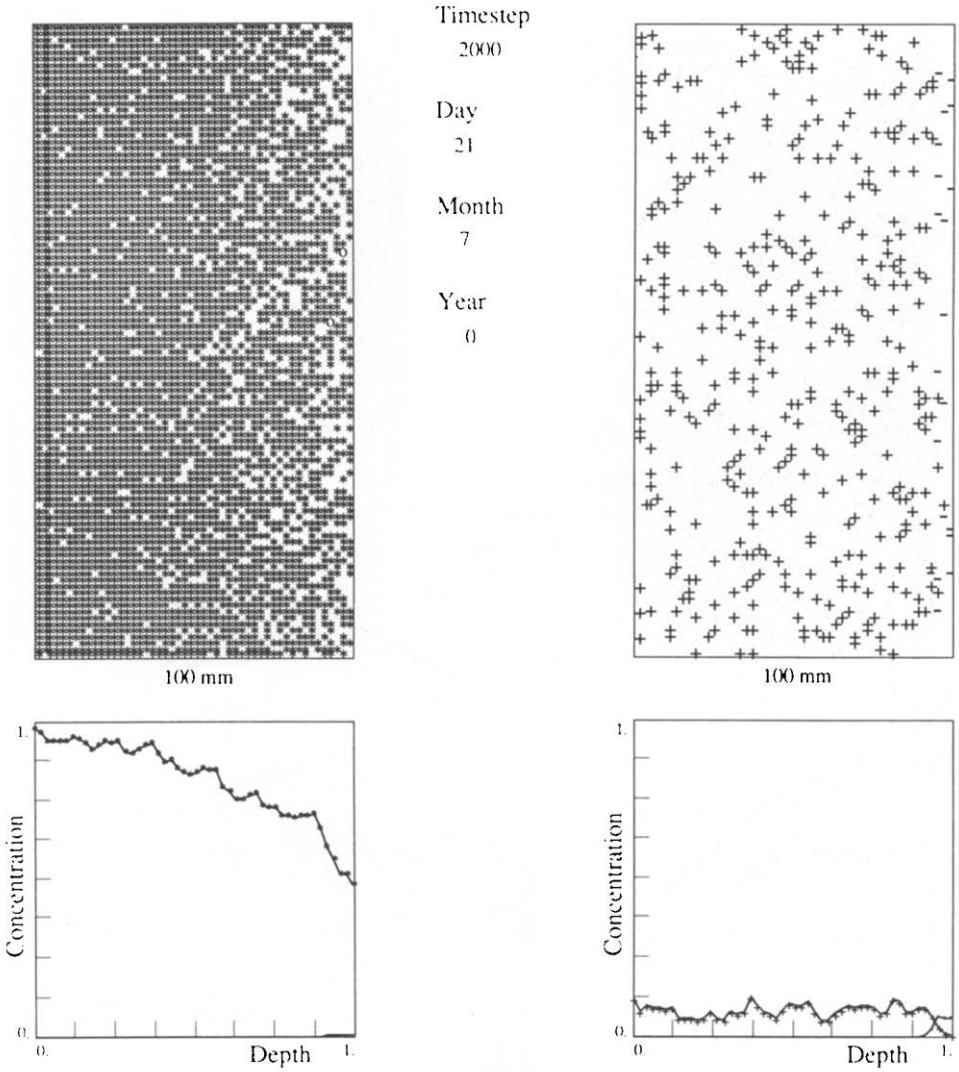

FIG. 5. Simulated behaviour of the carbonation reaction, $CO_2 + Ca(OH)_2 \rightarrow CaCO_3 + H_2O$, in a [illegible] depicts the transition between the uncontaminated region and the "carbonation zone," in which the transformation of $Ca(OH)_2$ (+) into $CaCO_3$ (−) is complete.

units guarantees that the spontaneous reaction (21) as implemented in the automaton is stoichiometrically correct. At the right-hand border, the boundary condition for water, representative of atmospheric relative humidity, is also determined by the isotherm. The corresponding boundary condition for CO_2 follows from its solubility and the amount of water present. These boundary conditions are

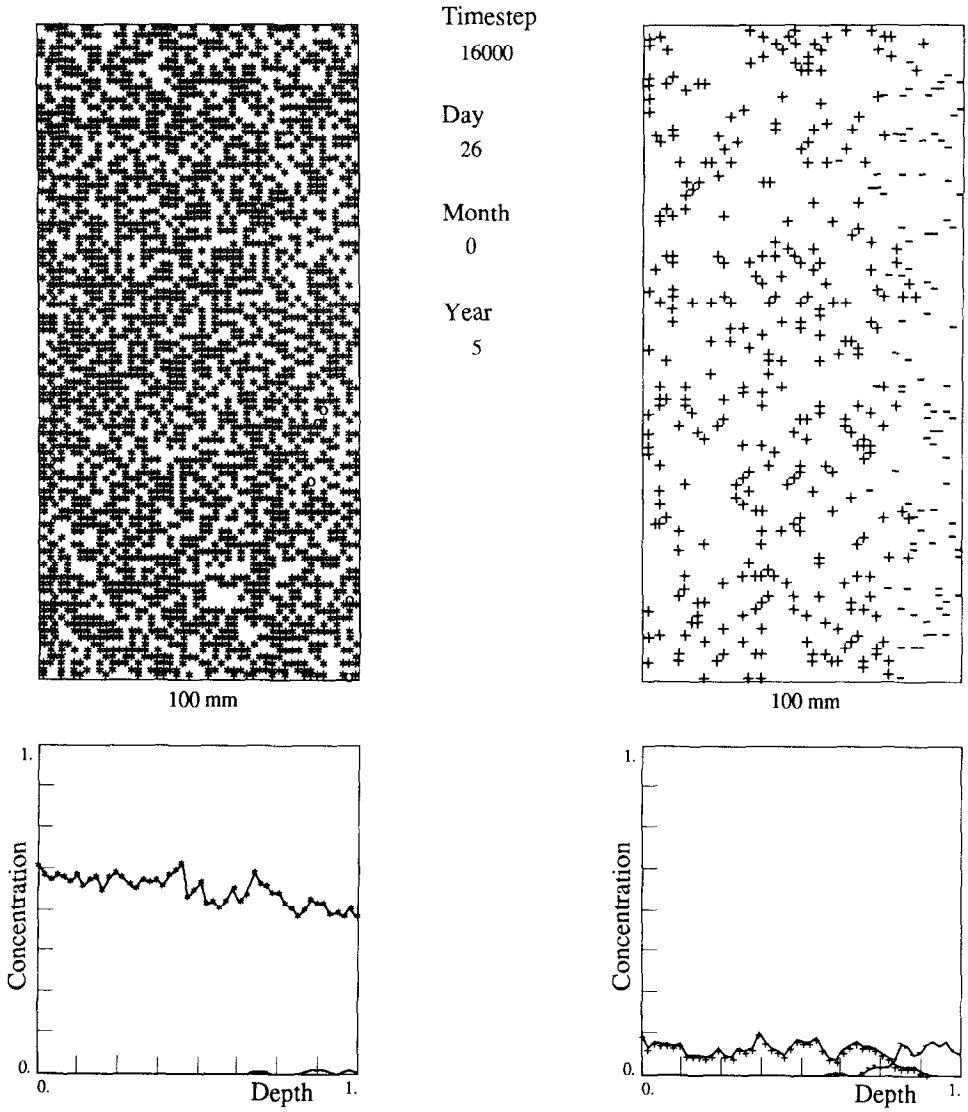

FIG. 5—*Continued*

imposed in the automaton by placing the appropriate number of particles of these species in the column at the right: the sum must represent the correct number of moles per unit volume at the surface. It is worth mentioning perhaps that in this application the relative quantities of the species are highly disparate: under typical conditions, the CO_2 boundary condition can be easily more than three orders of magnitude smaller than the boundary condition for water. The other borders respect zero flux conditions. Temperature is supposed constant, 20° C, for this simulation.

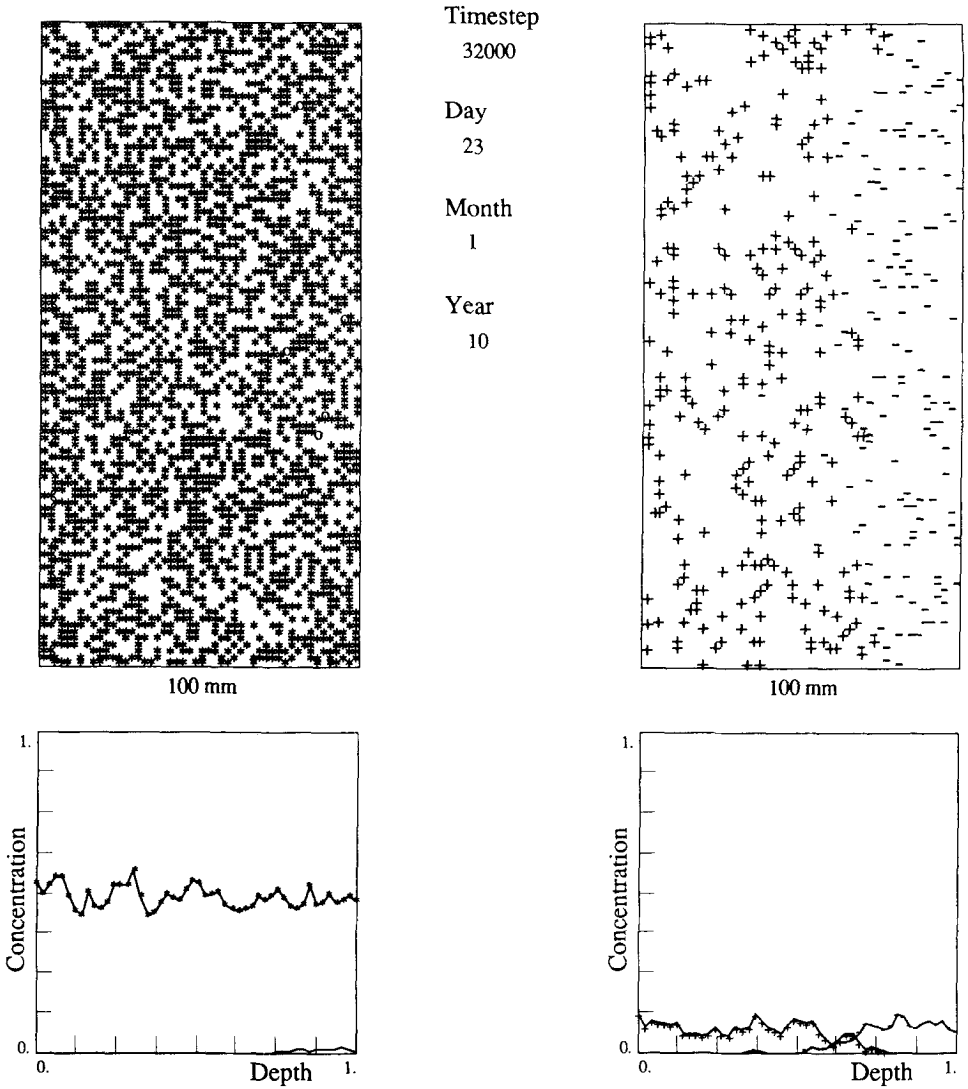

FIG. 5—*Continued*

Figure 5 shows the simulated behaviour of the carbonation reaction in a mortar specimen. The sample is initially saturated with water and dries in an atmosphere of CO_2 at a fixed relative humidity of 50%, emulating laboratory conditions. We see the equilibration of the water content with progressive timesteps as the simulated specimen dries. In addition, three distinct zones are visible: the "carbonated zone" in which the $Ca(OH)_2$ has been exhausted and the pH correspondingly diminished, the reaction "front," that zone in which reaction (21) continues to take place, and the innermost region where the CO_2 has not yet

arrived. With progressive timesteps we see the inward progress of the reaction as well as the accumulation of CO_2 behind the reaction front. The characteristics of these zones vary as a function of the parameters: a higher $Ca(OH)_2$ content yields a thinner reaction zone, for example.

5. Conclusion

In the present paper we have investigated a probabilistic cellular automaton model, using simple microscopic probabilistic dynamics to reproduce deterministic macroscopic behaviour. The realism of the implemented rules as reflections of microscopic physical phenomena is not the main goal; what is critical and perhaps the most difficult to achieve is that the cooperative effect of the local rules correctly reproduce the macroscopic physical observables. The states of the sites in the model are represented in bits, and the dynamics of the system are governed by a set of bit operations. In the model described in this article, the operations which cause the evolution of the sites are chosen by stochastic rules from among the set of possible bit operations.

We have presented a particular synchronous lattice gas model as a parallel algorithm for simulating diffusion. The deviation between the macroscopic description of this model and the discretized diffusion equation results from the simultaneous, independent displacements of the particles which respect an exclusion principle. It is not the only synchronous implementation possible, but it illustrates well the difference between asynchronous and synchronous dynamics and the problem of finding the right automaton rules to correctly simulate a given equation [16].

We have also demonstrated the use of cellular automata as modelling tools which facilitate the simulation of a complex physical process. The application presented here is a reaction-diffusion process in a porous medium (the carbonation of concrete).

References

1. S. Wolfram, *Rev. Mod. Phys.* **55**, 601 (1983).
2. J.-P. Rivet, M. Hénon, U. Frisch, and D. d'Humières, *Europhys. Lett.* (1988).
3. T. Toffoli and N. Margolus, *Cellular Automata Machines* (MIT Press, Cambridge, MA, 1987).
4. A. Clouqueur and D. d'Humières, *Complex Syst.* **1**, 585 (1987).
5. U. Frisch, B. Hasslacher, and Y. Pomeau, *Phys. Rev. Lett.* **56**, No. 14, 1505 (1986).
6. B. M. Boghosian and C. D. Levermore, *Complex Syst.* **1** (1987).
7. See the *Proceedings, NATO Workshop on Lattice Gas Methods for PDE's, Los Alamos, Sept. 1989*; *Phys. D* **47** (1991).
8. S. Wolfram, *J. Statist. Phys.* **45**, 471 (1986).
9. W. Feller, *An Introduction to Probability Theory and Its Applications* (Wiley, New York, 1964).
10. L. M. Brieger and E. Bonomi, in *Proceedings, 6th Symposium on Continuum Models and Discrete Systems, Dijon, France, 1989*, edited by G. A. Maugin (Longman Scientific and Technical, UK, 1991).

11. F. A. L. DULLIEN, *Porous Media–Fluid Transport and Pore Structure* (Academic Press, New York, 1979).
12. Z. P. BAZANT AND L. J. NAJJAR, *Cement and Concrete Research* **1**, 461 (1971).
13. L. M. BRIEGER AND F. H. WITTMANN, in *Proceedings, Int. Colloq. on Materials Science and Restoration, Esslingen, West Germany, 1989*, p. 635.
14. C. L. KAMP, P. E. ROELFSTRA, AND F. H. WITTMANN, in *Proceedings, IABSE Colloq., Delft, Holland, 1987*, p. 329.
15. C. L. KAMP, *Chantiers/Suisse* **19**, 419 (1988).
16. L. M. BRIEGER AND E. BONOMI, *Phys. D* **47**, 159 (1991).